1988

A Dimensionality Paradigm for Surface Interrogations

Christoph M. Hoffmann
Purdue University, cmh@cs.purdue.edu

Report Number:
88-837

A DIMENSIONALITY PRADIGM FOR SURFACE INTERROGATIONS

Christoph M. Hoffmann

CSD-TR-837
December 1988

A Dimensionality Paradigm for Surface Interrogations

Christoph M. Hoffmann*
Computer Science Department
Purdue University
West Lafayette, IN 47907

December 13, 1988

Abstract

We propose a paradigm for analyzing problems involving complex curved surfaces in a manner suitable for practical implementation. Rather than deriving closed-form expressions for certain surfaces and problems, we propose to reformulate the problem in a higher dimensional space with more variables but simpler equations, thus avoiding complex symbolic manipulation and numerically delicate operations.

1 Introduction

Many technical difficulties must be faced when creating the algorithmic infrastructure needed for solid modeling with curved surfaces. These difficulties suggest that it might be fruitful to reexamine some of the assumptions that underly the representations of curved surfaces and the strategies employed by the algorithms interrogating them. Specifically, operations on surfaces including offsetting and circular blending tend to lead to serious complications, and the machinery needed to derive explicit representations of the results is computationally expensive and numerically delicate. For

*Supported in part by NSF Grants CCR 86-19817 and DMC 88-07550, and by ONR Contract N00014-86-K-0465.

this reason, a number of approximation schemes have been advocated in the literature, including [6, 8, 17].

When these operations are reformulated in different spaces, however, they become very simple indeed. But these spaces have more than three dimensions, and the question arises whether the reformulation of the problem can be used directly as a surface representation in lieu of an equivalent parametric or implicit representation in familiar three space. There are many indications that this is indeed the case, and that doing so realizes substantial advantages. These advantages include:

1. The higher-dimensional representation has lower algebraic degree than an equivalent representation in three space would have, and is therefore easier to query numerically. Moreover, certain costly elimination steps that would be needed to find the representation in three space become unnecessary.

2. When creating the higher dimensional representation, fewer operations are performed on the numerical input data. Therefore, the resulting set of equations has coefficients that are more precise, and will yield results of greater accuracy than could be obtained otherwise.

3. In the higher-dimensional problem formulation, additional structural properties of the geometric operation are explicit. These properties help in applications such as motion planning or machining. For example, when offsetting a parametric surface f, we obtain simultaneously a projection function that associates with each point p on the offset surface its projection p_f on f and the parametric coordinates of p_f.

In this paper, we examine the construction of offset surfaces, of Voronoi surfaces, and of variable radius blending surfaces as an example of this approach, and demonstrate that the higher dimensional formulation can be used directly for surface intersection.

2 Surface Intersections

In [10], Geisow argues that the evaluation of surface intersection is reducible to evaluating a plane curve $h(u, v) = 0$. In particular, the intersection of the

implicit surface

$$f(x, y, z) = 0$$

with the *parametric* surface g given by

$$x = g_1(u, v) \qquad y = g_2(u, v) \qquad z = g_3(u, v)$$

is readily seen in birational correspondence with the plane curve

$$f(g_1, g_2, g_3) = h(u, v) = 0$$

See, e.g., [7, 16]. The intersection of two parametric surfaces can be similarly mapped to a plane curve after first implicitizing one of the surfaces, e.g., [18], a procedure always possible albeit not necessarily efficient. Even the intersection of two implicit surfaces f and g can be so approached, by finding in the ideal of the two surfaces a *monoid* $\bar{g}$ that contains the intersection and is readily parameterized, [12]. Related approaches to the intersection of two implicit surfaces are given in [1, 9].

While mathematically tidy and conceptually appealing, evaluating surface intersection in this way is beset by a number of practical difficulties, including the following:

1. Implicitizing a parametrically defined surface entails substantial symbolic computation for degrees higher than cubic [19]. Moreover, in the absence of more sophisticated techniques such as [4, 5], the derived implicit form may have extraneous factors that are difficult to eliminate.

2. Substitution of the parametric functions into the implicit form, although conceptually straightforward, is numerically delicate, and can lead to substantial errors [15].

3. By Bezout's theorem, the degree of h is equal to the product of the degrees of the intersecting surfaces. Thus, with the resulting high algebraic degrees numerical difficulties arise even when evaluating h at some given point p.

Therefore, what looks attractive from a theoretical vantage point, may not work at all when implemented, and alternative approaches should be developed.

We propose as practical alternative a dimensionality paradigm that seeks to keep the problem manageable by reformulating the computation at hand. Specifically, we formulate an equivalent problem in higher dimensional space, using more variables and more, but simpler equations. We demonstrate this paradigm intersecting a number of mathematically complicated surfaces.

In [2] an algorithm was presented for tracing the intersection of two surfaces. The algorithm presented there in Section 3 can be applied without any essential modification to surface intersection in all dimensions. It repeats the following three steps, for $i = 0, 1, 2, ...$

1. Given an initial point estimate q_i on the curve, refine it using Newton iteration to a point p_i.
2. At p_i, construct a local approximant $\mathbf{r}(s)$, to second or third order.
3. Choose adaptively a step size s_{i+1}, and derive a new point estimate $q_{i+1} = \mathbf{r}(s_{i+1})$.

In the examples of this paper, we compute a second order approximant to the curve and choose a step size such that the contribution of the second order term is not more than 10 percent. With this proviso, typically 2 or 3 Newton iteration steps are performed to refine the next curve point estimate to ten digits precision.

3 Offset Surfaces

Given a surface $f = 0$, its *r-offset* consists of the points

$$\mathrm{Off}(f, r) = \{p \mid \mathrm{d}_f(p) = r\}$$

where $\mathrm{d}_f(p)$ is the Euclidian distance of the point p from the surface $f = 0$. Informally, at each regular surface point p of f we erect the surface normal and on it, at distance r in either direction, mark a point. Both points so obtained belong to $\mathrm{Off}(f, r)$.

In general, the offset surface has two sheets in real affine space, one sheet formed by the points offset from the surface in one direction, the other sheet formed by the points offset in the other normal direction. If f is an irreducible algebraic surface, both sheets together will in general

be described by a single, irreducible algebraic equation, evidencing the fact that both belong to the same irreducible surface. Exceptions to this include the offsets of a sphere that consist of two spheres, each separately definable by an algebraic equation.

In the traditional offset formulation, e.g., [8], the second sheet does not appear to be constructed. The formulation involves a square root, to compute a unit normal vector, and, by convention, the positive root is assumed. But from an algebraic point of view both roots must be accounted for when implicitizing the surface so defined, hence both sheets would be represented in the *implicit* equation entailed by the method.

Offset surfaces can be defined mathematically with the envelope theorem from differential geometry [20] that states that the envelope of a parameterized family $S(\alpha) = 0$ of surfaces are the points satisfying the system of equations

$$\begin{aligned} S(\alpha) &= 0 && (1) \\ \partial S(\alpha)/\partial u &= 0 && (2) \end{aligned}$$

With α a vector of m independent parameters, the equations (2) are the m first-order partial derivatives of $S(\alpha)$ by each component u of α. Thus the system consists of $m + 1$ equations.

If the parameters α are not all algebraically independent, e.g., are the coordinates of points on another surface, then the equations (2) must be replaced by the *directional derivatives* of $S(\alpha)$ and the defining dependency equations among the parameters must be added as additional constraints.

We formulate the r-offset of f as the envelope of a family of spheres with radius r whose centers are constrained to lie on the surface. Figure 1 illustrates this concept in two dimensions. Assume that the surface f is given in parametric form as

$$\begin{aligned} x &= f_1(s,t) \\ y &= f_2(s,t) \\ z &= f_3(s,t) \end{aligned}$$

Then its r-offset is described by the system

$$\begin{aligned} S(s,t) &= 0 \\ \partial S(s,t)/\partial s &= 0 \\ \partial S(s,t)/\partial t &= 0 \end{aligned} \qquad (3)$$

where

$$S(s,t) = (x - f_1(s,t))^2 + (y - f_2(s,t))^2 + (z - f_3(s,t))^2 - r^2$$

Next, assume that the surface is given by an implicit equation $f(x,y,z) = 0$. Let $p = (u_1, u_2, u_3)$ be a regular point on f, and let $\nabla f(p) = (a,b,c)$ be the surface gradient at p. We construct the equations for the r-offset by taking spheres of radius r centered on the surface:

$$\begin{aligned} S: \quad (x-u_1)^2 + (y-u_2)^2 + (z-u_3)^2 - r^2 &= 0 \\ f(u_1,u_2,u_3) &= 0 \end{aligned}$$

and forming the directional derivatives by multiplying the vector of partials of S by the u_i with two linearly independent vectors perpendicular to the gradient at p. For example, with the two perpendiculars taken as $(-b,a,0)$ and $(-c,0,a)$, we obtain the directional derivatives

$$S_1 = \nabla S \cdot (-b,a,0)$$

and

$$S_2 = \nabla S \cdot (-c,0,a)$$

where

$$\nabla S = (\frac{\partial S}{\partial u_1}, \frac{\partial S}{\partial u_2}, \frac{\partial S}{\partial u_3})$$

So, the r-offset of f is described by the system

$$\begin{aligned} S &= 0 \\ f &= 0 \\ S_1 &= 0 \\ S_2 &= 0 \end{aligned} \tag{4}$$

We could have chosen a different pair of perpendiculars, e.g., $(-b,a,0)$ and $(b-c, a-b, c-a)$. Note, however, that the choice of perpendiculars may introduce extraneous solutions, [13], Chapter VII. For example, the two perpendiculars $(-b,a,0)$ and $(-c,0,a)$ will introduce the extraneous factor x.

In principle, we may recover the *implicit* equation of the r-offset from System (3) by eliminating both s and t, and from System (4) by eliminating u_1, u_2, and u_3. If elimination is done using resultant methods, the final equation may contain additional extraneous factors. These factors may be

difficult to find and eliminate. Alternatively, the elimination can be attempted using Gröbner basis techniques, e.g., as described in [13], avoiding the extraneous factors problem. Except for very simple situations, however, one must expect that both approaches require very long running times.

An additional difficulty, not normally addressed in the literature, is the fact that we usually do not have exact surface equations to begin with. So, the symbolic computations either work with rational coefficient approximations of uncertain accuracy, or else incur arithmetic errors that have not been analyzed in the literature and thus cannot be predicted with confidence. In practical settings, therefore, even if the computation times were negligible, the value of eliminating the problem parameters would have to be doubted.

Example 1: We offset a quadric surface $f = 0$ by the distance 2 and intersect it with a quartic surface $h = 0$. The implicit equation of the offset of f has degree 8, so the intersection curve with h, when properly mapped, must result in a plane curve of degree 32 which will be moderately hard to handle numerically. In contrast, the system to be formulated consists of equations with maximum degree 4 and is quite easy to treat numerically.

We formulate the offset equations first, with f the ellipsoid $16x^2+36y^2+9z^2-144=0$. The ellipsoid is centered at the origin, and its axes are 3, 2, and 4, respectively.

$$\begin{aligned} (x-u_1)^2+(y-u_2)^2+(z-u_3)^2-4 &= 0 \\ 16u_1^2+36u_2^2+9u_3^2-144 &= 0 \\ 36u_2(x-u_1)-16u_1(y-u_2) &= 0 \\ 9u_3(x-u_1)-16u_1(z-u_3) &= 0 \end{aligned} \tag{5}$$

To this system, we add the equation of the quartic surface

$$(x^2-10x+y^2+z^2+21)^2-20(x^2-10x+29)-16(y^2-z^2)-48x-176=0$$

The shapes of the quartic and of the ellipsoid are shown in Figure 2. We trace the intersection directly from the five equations. The trace not only constructs the intersection curve, as the points (x, y, z), it also constructs simultaneously the *projection* (u_1, u_2, u_3) of this curve onto the ellipsoid. This information is useful in compliant motion applications and in numerically controlled machining problems. A graphical rendering of both curves is shown in Figure 3. $\diamond$

Example 2: We consider offsetting a Bezier bicubic patch f by a distance 1 and intersecting it with a quadratic surface $h = 0$. The implicit

equation of the bicubic patch is of degree 18, so its offset will be of degree 36 or higher. Thus, the intersection curve would have to be mapped to a plane algebraic curve of degree 72 or higher and would pose very difficult numerical evaluation problems.

Let the bicubic patch be given by the control points

$$\begin{pmatrix} (0,0,0) & (-1,1,1) & (0,2,1) & (0,3,0) \\ (1,0,1) & (1,1,0) & (1,2,1) & (1,4,-1) \\ (2,0,1) & (2,1,-1) & (2,2,0) & (2,3,-1) \\ (3,0,0) & (3,1,0) & (3,2,1) & (3,3,0) \end{pmatrix}$$

from which we obtain the following parametric equations

$$\begin{aligned} x &= f_1(s,t) = 3t(t-1)^2(s-1)^3 + 3s \\ y &= f_2(s,t) = 3s(s-1)^2t^3 + 3t \\ z &= f_3(s,t) = -3s(s^2-5s+5)t^3 - 3(s^3+6s^2-9s+1)t^2 \\ &\quad +(6s^3+9s^2-18s+3)t - 3s(s-1) \end{aligned}$$

The patch is shown graphically in Figure 4. Its offset would be defined by

$$(x-f_1)^2 + (y-f_2)^2 + (z-f_3)^2 - 1 = 0$$

and its two partial derivatives by s and by t. We choose for h the sphere $2(x^2+y^2+z^2) - 6x - 6y - 4z + 9 = 0$, of radius 1 centered at $(1.5, 1.5, 1.0)$.

A trace of the resulting system is shown in Figure 5. The trace also delivers (s,t) values for each intersection point. These are the parameter coordinates of the projection of the intersection point onto the bicubic surface. $\diamond$

Note that we can apply this method also to intersecting two offset surfaces, tracing simultaneously the intersection curve and its two projections.

4 Voronoi Surfaces

We are given two surfaces f and g, and consider the locus of all points in space that have equal distance from either surface. The resulting point set is the *Voronoi surface* of f and g, formally defined by

$$\mathrm{Vor}(f,g) = \{p = (x,y,z) \mid \mathrm{d}_f(p) = \mathrm{d}_g(p)\}$$

Note the analogy with Voronoi diagrams. We will consider these surfaces in the next section as a means for defining certain blending surfaces.

We adopt the following notational conventions: The surfaces to which we seek the Voronoi surface are $f = 0$ and $g = 0$. When a surface is given parametrically, we index the parametric functions by numbers and the parameters by the surface name. Thus, a parametric surface f would be given as

$$x = f_1(s_f, t_f), \quad y = f_2(s_f, t_f), \quad z = f_3(s_f, t_f)$$

Moreover, a sphere centered on a surface f is denoted S_f.

We define the Voronoi surface with help of offsets from each surface by a variable distance r. Thus, if the surfaces are given parametrically, as

$$\begin{array}{lll} x = f_1(s_f, t_f) & y = f_2(s_f, t_f) & z = f_3(s_f, t_f) \\ x = g_1(s_g, t_g) & y = g_2(s_g, t_g) & z = g_3(s_g, t_g) \end{array}$$

then the Voronoi surface may be specified by

$$\begin{array}{rcl} S_f : (x - f_1)^2 + (y - f_2)^2 + (z - f_3)^2 - r^2 & = & 0 \\ \partial S_f / \partial s_f & = & 0 \\ \partial S_f / \partial t_f & = & 0 \\ S_g : (x - g_1)^2 + (y - g_2)^2 + (z - g_3)^2 - r^2 & = & 0 \\ \partial S_g / \partial s_g & = & 0 \\ \partial S_g / \partial t_g & = & 0 \end{array} \tag{6}$$

This system is the juxtaposition of the offsets from both f and g by a common but unspecified distance r. With r ranging over all possible distances, we have a description of the Voronoi surface in an eight dimensional space. Similarly, when f and g are given implicitly, their Voronoi surface is described by eight equations in ten variables.

The implicit equation of the Voronoi surface could be recovered, in principle, by elimination of s_f, t_f, s_g, t_g, and r from the system, a proposition that is hardly practical for all but the simplest surfaces. Voronoi surfaces typically have high degree, but special situations can be identified in which the Voronoi surface is very simple. For instance, the Voronoi surface of two cylinders of equal radius with skew axes passing each other is a hyperbolic paraboloid. Moreover, the Voronoi surface of a cylinder and an inclined plane consists of two elliptic cones.

Example 3: We intersect the Voronoi surface of f and g with a third surface h. For f, we choose the bicubic patch of Example 2 and use for g the ellipsoid $4(2x-3)^2+9(2y-3)^2+36(z-1)^2-36=0$, centered at $(1.5,1.5,1.0)$ with axis lengths 1.5, 1.5, and 1. The Voronoi surface is thus described by

$$\begin{array}{rrcl} S_f: & (x-f_1)^2+(y-f_2)^2+(z-f_3)^2-r^2 &=& 0 \\ & \partial S_f/\partial s &=& 0 \\ & \partial S_f/\partial t &=& 0 \\ S_g: & (x-v_1)^2+(y-v_2)^2+(z-v_3)^2-r^2 &=& 0 \\ g: & 4(2v_1-3)^2+9(2v_2-3)^2+36(v_3-1)^2-9 &=& 0 \\ & 9(2v_2-3)(x-v_1)-4(2v_1-3)(y-v_2) &=& 0 \\ & 36(v_3-1)(x-v_1)-8(2v_1-3)(z-v_3) &=& 0 \end{array} \qquad (7)$$

We intersect the surface with the elliptic cylinder

$$h: 1250x^2-3750x+4050y^2-10530y+5607=0$$

whose axis is parallel to the z-axis through the point $(1.5,1.3,0)$. Figure 6 shows a trace of the intersection curve and its two projections onto f and g. $\diamond$

5 Variable Radius Blends

Given two surfaces f and g, a *blending surface* is a surface F that intersects both f and g tangentially along some curves. A *constant radius blend* is a blending surface that has a family of principal curvature lines consisting of circles of fixed radius. A *variable radius* blend, finally, is a blending surface that has a family of principal curvature lines consisting of circles whose radius may vary. Constant radius and variable radius blends are used in designing mechanical parts.

A *canal surface* is the envelope surface of a family of spheres with fixed or varying radius whose centers are constrained to lie on a space curve. The space curve is called the *spine* of the canal surface. Canal surfaces have been studied primarily in differential geometry, and a key theorem, due to Monge, implies a that variable radius blending surface is a canal surface, i.e., the envelope of a family of spheres whose centers are constrained to lie on a space curve.

Monge's theorem gives a way for defining constant radius blending surfaces with precision. Such a blend is simply the canal surface that envelopes the family of spheres of constant radius r whose centers lie on the curve $\mathrm{Off}(f,r) \cap \mathrm{Off}(g,r)$. Such blending surfaces have been considered in [17].

There has been no similarly precise definition for variable radius blends, primarily because of the difficulty to quantify the radius variation of such a surface. For example, the procedural definition given in [14] is unsatisfactory because the algorithm for defining the radius variation contains unspecified degrees of freedom that affect the shape of the final surface. For this reason, we have made in [6] the following definition of a variable radius blend for the surfaces f and g:

> Consider the intersection $\mathrm{Vor}(f,g) \cap h$ of the Voronoi surface $\mathrm{Vor}(f,g)$ of f and g with a *reference* surface h. Then a variable radius blend of f and g is the envelope of the family of spheres whose centers lie on $\mathrm{Vor}(f,g) \cap h$ and whose radii are such that each sphere touches both f and g.

Hence, $\mathrm{Vor}(f,g) \cap h$ is the spine of the variable radius blend. Moreover, we can project each point p of the intersection onto the two surfaces, obtaining the points p_f and p_g at which the sphere centered at p touches f and g. A section of the variable radius blend can then be constructed in the plane spanned by the three points p, p_f, and p_g and is a circle of radius r centered at p. This circle is a principal line of curvature.

We construct a higher dimensional representation of a variable radius blending surface, from the definition given above. To this end, we will derive a system of equations in 11–15 variables defining the surface. The exact number of equations and variables depends on how the original surfaces were specified. See also the example below. It would be difficult to imagine that elimination of the additional variables could succeed in efficiently deriving an implicit equation for this blend. In [6] we have explored the alternative of approximating a variable radius blend with quartic surface elements.

As first step, we formulate the intersection curve of the Voronoi surface $\mathrm{Vor}(f,g)$ with some reference surface h. We alter the system (6) by renaming the variables x, y, and z to u_1, u_2, and u_3, respectively. Assume that the reference surface is given by

$$x = h_1(s_h, t_h),\ y = h_2(s_h, t_h),\ z = h_3(s_h, t_h)$$

Then we adjoin to the system with the renamed variables the equations $u_i = h_i(s_h, t_h)$. The enlarged system specifies that the point (u_1, u_2, u_3) must lie on the intersection $\mathrm{Vor}(f, g) \cap h$.

The next step in defining the variable radius blend is to formulate a description of the spheres that are centered on the intersection of the Voronoi and the reference surface, and have a radius such that they touch both f and g. The center of a sphere in this family is simply the point (u_1, u_2, u_3). Its radius must be r, since this is the distance of the center from both surfaces to be blended. Hence we add the equation

$$S_h : (x - u_1)^2 + (y - u_2)^2 + (z - u_3)^2 - r^2 \quad = \quad 0$$

to describe the family of spheres whose envelope is the desired blending surface.

In order to define the envelope of the family, we must add an equation that is the derivative of S_h in the tangent direction. At the point (u_1, u_2, u_3), the tangent direction to the spine is given by the cross product of the surface normals of $\mathrm{Vor}(f, g)$ and of h. The normal to h is easily specified as the cross product

$$N_h = (\frac{\partial h_1}{\partial s_h}, \frac{\partial h_2}{\partial s_h}, \frac{\partial h_3}{\partial s_h}) \times (\frac{\partial h_1}{\partial t_h}, \frac{\partial h_2}{\partial t_h}, \frac{\partial h_3}{\partial t_h})$$

The normal to $\mathrm{Vor}(f, g)$ is obtained as follows. Consider the lines connecting the point $p = (u_1, u_2, u_3)$ on the Voronoi surface with its projections $p_f = (f_1, f_2, f_3)$ and $p_g = (g_1, g_2, g_3)$, where the coordinate functions f_i and g_i are evaluated at (s_f, t_f) and at (s_g, t_g), respectively. Since the lines (p, p_f) and (p, p_g) are perpendicular to f and g, respectively, it follows that the tangent plane to the Voronoi surface at p is the bisecting plane of the two lines [21], as illustrated in Figure 7. Since the vectors $\overline{(p, p_f)}$ and $\overline{(p, p_g)}$ have equal length, the normal to the Voronoi surface at p is therefore the vector

$$N_v = \overline{(p, p_f)} - \overline{(p, p_g)} = (f_1 - g_1, f_2 - g_2, f_3 - g_3)$$

We compute the cross product of the two normals and obtain the tangent vector to the intersection curve at p as

$$T = N_h \times N_v$$

So, the directional derivative of S_h, to be adjoined to the system, is

$$D = (\frac{\partial S_h}{\partial u_1}, \frac{\partial S_h}{\partial u_2}, \frac{\partial S_h}{\partial u_3}) \cdot T = 0$$

This gives us as final system describing the variable radius blend

$$\begin{aligned}
S_f: \quad (u_1-f_1)^2+(u_2-f_2)^2+(u_3-f_3)^2-r^2 &= 0\\
\partial S_f/\partial s_f &= 0\\
\partial S_f/\partial t_f &= 0\\
S_g: \quad (u_1-g_1)^2+(u_2-g_2)^2+(u_3-g_3)^2-r^2 &= 0\\
\partial S_g/\partial s_g &= 0\\
\partial S_g/\partial t_g &= 0\\
u_1 &= h_1(s_h,t_h)\\
u_2 &= h_2(s_h,t_h)\\
u_3 &= h_3(s_h,t_h)\\
S_h: \quad (x-u_1)^2+(y-u_2)^2+(z-u_3)^2-r^2 &= 0\\
D &= 0
\end{aligned} \tag{8}$$

We illustrate the method with an example.

Example 4: We construct a variable radius blend to the surfaces f and g of Example 3. We use as reference surface the surface h of that example. Then the equations describing the blending surface are

$$\begin{aligned}
S_f: \quad (u_1-f_1)^2+(u_2-f_2)^2+(u_3-f_3)^2-r^2 &= 0\\
\partial S_f/\partial s &= 0\\
\partial S_f/\partial t &= 0\\
S_g: \quad (u_1-v_1)^2+(u_2-v_2)^2+(u_3-v_3)^2 &= 0\\
g: \quad 4(2v_1-3)^2+9(2v_2-3)^2+36(v_3-1)^2-9 &= 0\\
9(2v_2-3)(u_1-v_1)-4(2v_1-3)(u_2-v_2) &= 0\\
36(v_3-1)(u_1-v_1)-8(2v_2-3)(u_3-v_3) &= 0\\
h: \quad 1250u_1^2-3750u_1+4050u_2^2-10530u_2+5607 &= 0\\
S_h: \quad (x-u_1)^2+(y-u_2)^2+(z-u_3)^2-r^2 &= 0\\
(\partial S_h/\partial u_1, \partial S_h/\partial u_2, \partial S_h/\partial u_3)\cdot T &= 0
\end{aligned}$$

where T is

$$T = (250u_1-375,\ 810u_2-1053,\ 0)\times(v_1-f_1,\ v_2-f_2,\ v_3-f_3)$$

These equations differ somewhat from System (8) because g and h are given implicitly rather than parametrically. To obtain a visual impression of the surface, we intersect the blend with planes through the axis of symmetry of h, given by

$$\cos(\omega)(10x-13)+\sin(\omega)(10y-15)=0$$

for several angles ω. The resulting curves are approximately circular but are not circles in general. All intersection curves are shown in Figure 8, along

Example	Dimensions	Highest Surf. Deg.	Estimated Curve Deg.	Time
1	6	4	32	1.8 sec
2	5	12	$\geq$72	2.1 sec
3	9	12	$\geq$72	5.1 sec
4	12	12	$\geq$144	9.7 sec

Table 1: Time to Generate One Point and Curve Approximant

with the two curves at which the blend is tangent to the bicubic surface and to the ellipsoid. $\diamond$

6 Degrees and Timings

We have demonstrated that certain surface operations can be formulated straightforwardly in higher dimensional spaces, and that such formulations can be used directly in surface interrogation. One advantage of this paradigm is its success in coping with curves and surfaces of very high algebraic degree.

The time needed to generate points and local curve approximants of second order are shown in the table. Also shown are the number of variables of the problem formulation and a conservative estimate of the degree of the curves traced. The time to generate a point grows with the problem dimension and with the highest degree of the equations in the problem.

The curve degrees were estimated as follows: By Bezout's theorem, the intersection degree equals the product of the degrees of the intersecting surfaces. Implicitization shows that the ellipsoid offset has degree 8. The bicubic patch has degree 18. An offset and a Voronoi surface constructed from a surface of degree n should have a degree at least $2n$. Likewise, the variable radius blend should have a degree at least double the spine degree.

All measurements were taken on a Sun 3/60. The current implementation is not optimized in any way, and much performance improvements could be obtained by replacing the evaluation routines with more sophisticated schemes. There is also a trade-off between the step size and the

number of Newton iterations needed to refine the new point estimate to the desired precision.

The linear systems arising as part of the trace algorithm were solved using the singular value decomposition routines of LINPACK.

Acknowledgements

Chris Scherbert implemented the higher dimensional version of the curve tracing software. The three dimensional version was originally implemented by Bob Lynch. Franz-Erich Wolter pointed out [21] to me and its implications for the Voronoi surface.

7 References

1. S. Abhyankar and C. Bajaj (1987), "Automatic Rational Parameterization of Curves and Surfaces IV: Algebraic Space Curves," *ACM Trans. on Graphics*, to appear.

2. C. Bajaj, C. Hoffmann, J. Hopcroft, and R. Lynch (1988), "Tracing Surface Intersections," *Computer Aided Geometric Design 5*, 285–307.

3. W. Böhm, G. Farin, and J. Kahmann (1984), "A Survey of Curve and Surface Methods in CAGD", *Computer Aided Geometric Design 1*, 1–60.

4. B. Buchberger (1985), "Gröbner Bases: An Algorithmic Method in Polynomial Ideal Theory," in *Multidimensional Systems Theory*, N. K. Bose, ed., D. Reidel Publishing Co., 184–232.

5. B. Buchberger, G. Collins, and B. Kutzler (1988), "Algebraic Methods for Geometric Reasoning," *Annl. Reviews in Comp. Science*, Vol. 3.

6. V. Chandru, D. Dutta, C. Hoffmann (1989), "Variable Radius Blending with Cyclides," *to appear.*

7. R. Farouki (1986), "Trimmed Surface Algorithms for the Evaluation and Interrogation of Solid Boundary Representation," *IBM J. Res. and Dev. 31*, 314–334.

8. R. Farouki (1986), "The Approximation of Nondegenerate Offset Surfaces," *Comp. Aided Geometric Design 3*, 15–43. Clarendon Press, Oxford, 363–385.

9. T. Garrity and J. Warren (1987), "On Computing the Intersection of a Pair of Algebraic Surfaces," *Comp. Aided Geometric Design*, to appear.

10. A. Geisow (1986), "Surface Interrogation," *Ph.D. Diss.*, School of Computing and Accountancy, Univ. of East Anglia.

11. G. Golub and C. van Loan (1983), *Matrix Computations*, Johns Hopkins Press.

12. C. Hoffmann (1987), "Algebraic Curves," in *Mathematical Aspects of Scientific Software*, J. Rice, ed., IMA Volumes in Math. and Applic., Springer Verlag, 101–122.

13. C. Hoffmann (1989) *Geometric and Solid Modeling*, Chapter 7. Morgan Kaufmann Publishers, to appear mid 1989.

14. J. Pegna (1988), "Variable Sweep Geometric Modeling," PhD Diss., Mech. Engr., Stanford Univ.

15. P. Prakash and N. Patrikalakis (1988), "Algebraic and Rational Polynomial Surface Intersections," *Computer Vision, Graphics, and Image Proc.*, to appear.

16. M. Pratt and A. Geisow (1986), "Surface/Surface Intersection Problems," in *The Mathematics of Surfaces*, J. Gregory, ed., Oxford University Press, 117–142.

17. J. Rossignac and A. Requicha (1984), "Constant Radius Blending in Solid Modeling," *Comp. Mech. Engr. 3*, 65–73.

18. T. Sederberg (1983), "Implicit and Parametric Curves and Surfaces for Computer Aided Geometric Design," *Ph.D. Diss.*, Mech. Engr., Purdue University

19. T. Sederberg and S. Parry (1986), "A Comparison of Curve Intersection Algorithms," *Comp. Aided Geometric Design 18*, 58–63.

20. M. Spivak (1975), *A Comprehensive Introduction to Differential Geometry*, Publish or Perish, Inc., Wilmington, Del. Vol. III, 255-263.

21. F.-E. Wolter (1985), "Cut Loci in Bordered and Unbordered Riemannian Manifolds," PhD Diss., Math., Tech. University Berlin, West Germany.

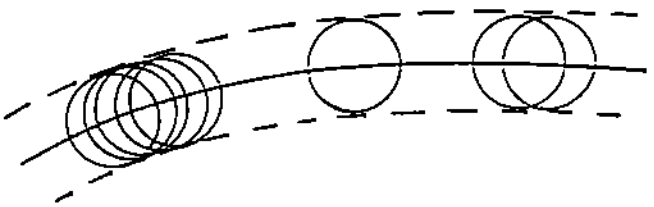

Figure 1: Curve Offset as Envelope

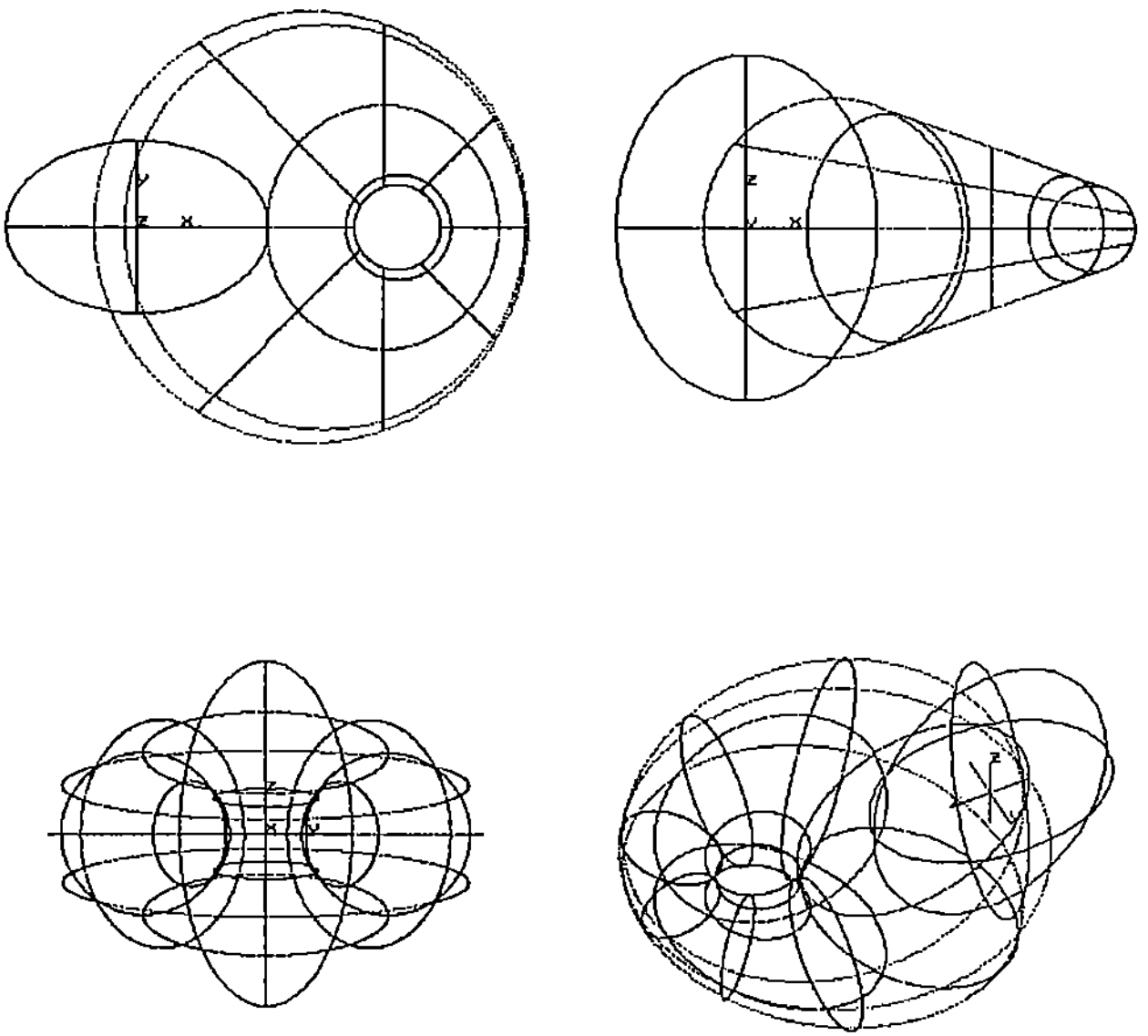

Figure 2: Ellipsoid and Quartic of Example 1

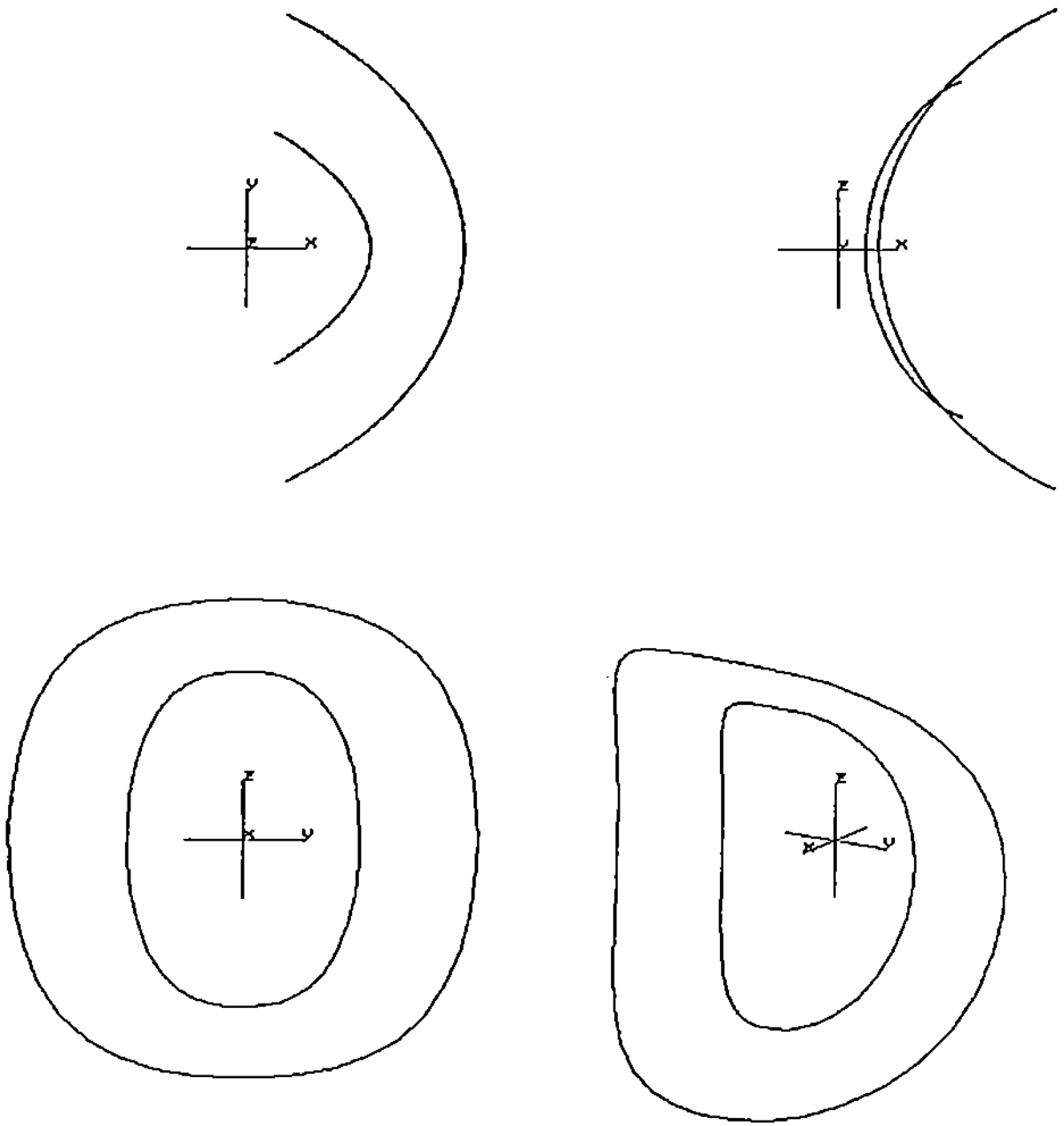

Figure 3: Intersection Curve of Example 1, and its Projection onto Ellipsoid

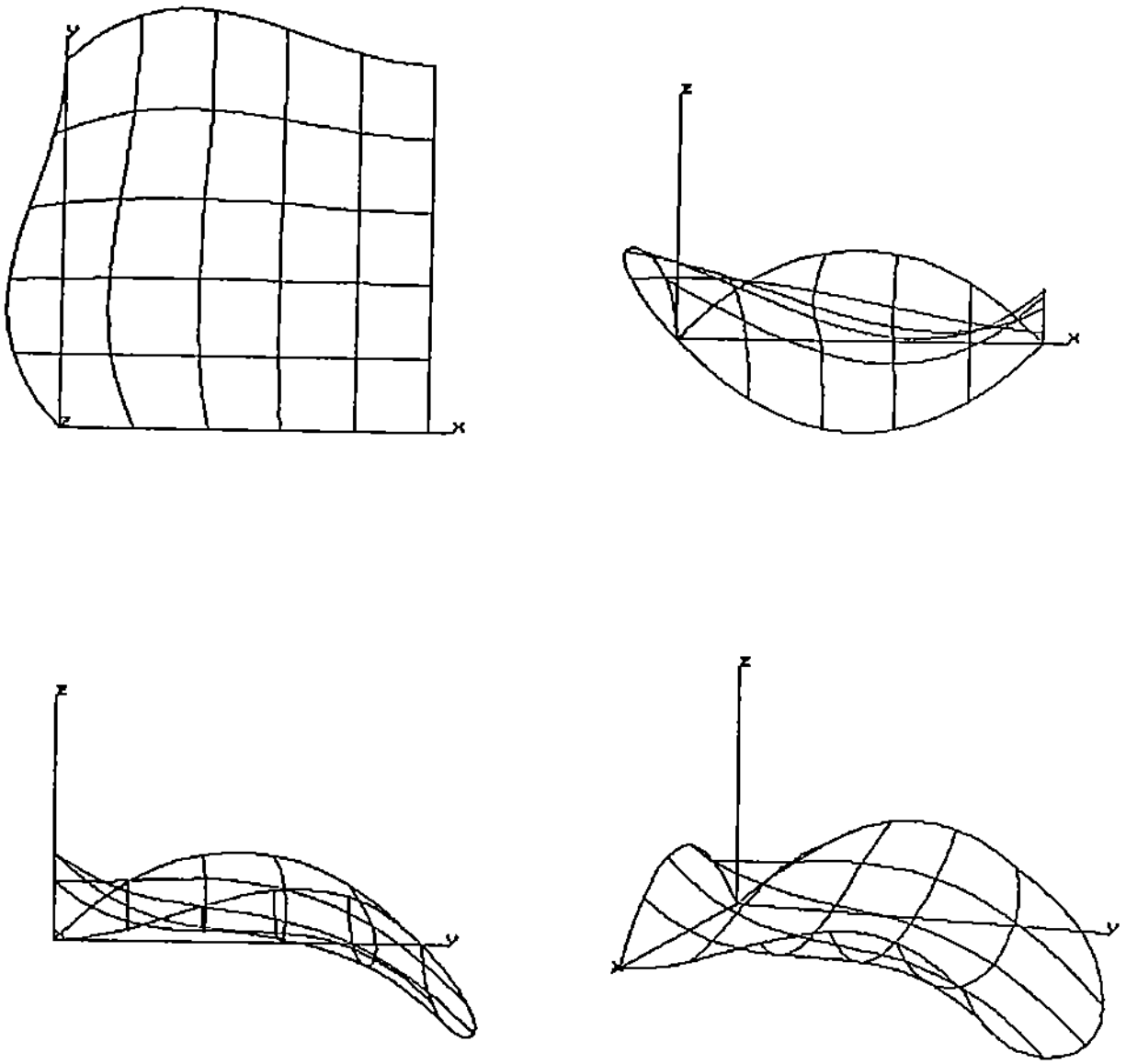

Figure 4: Bicubic Patch of Example 2 to be Offset

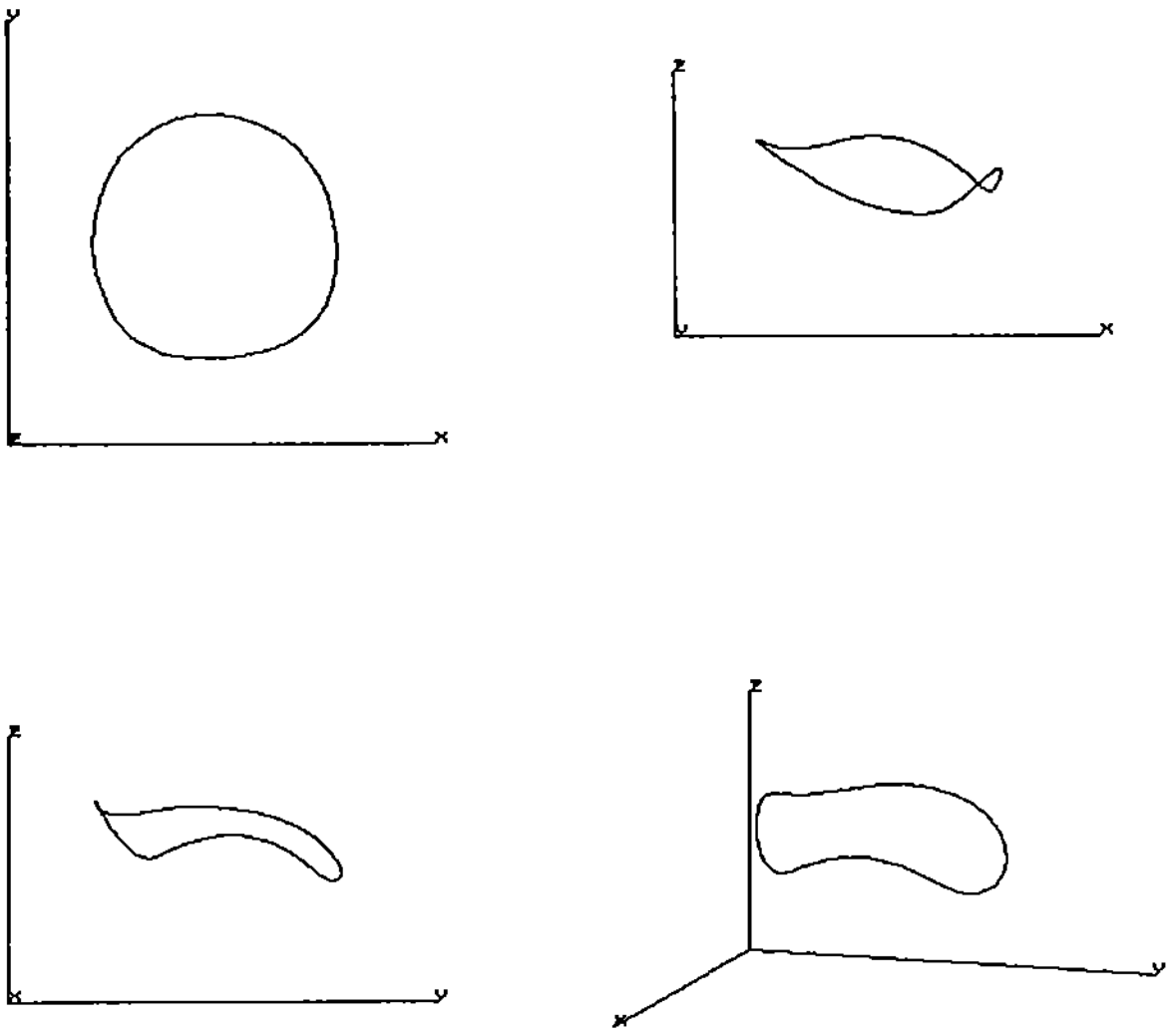

Figure 5: Offset of Bicubic Patch Intersected with Sphere, and its Projection in Parameter Space

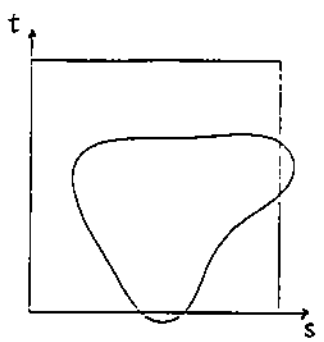

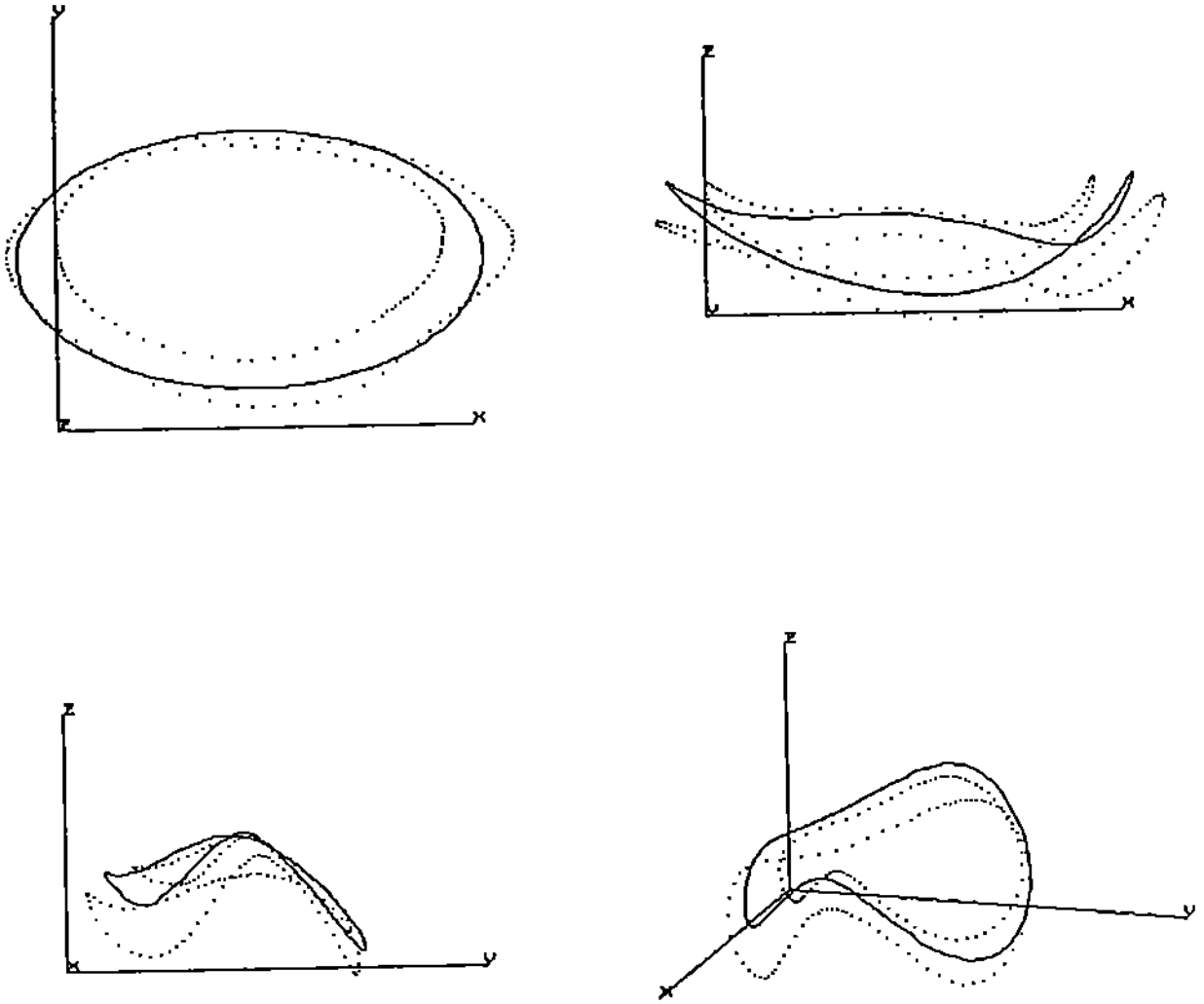

Figure 6: Intersection with a Voronoi Surface and Projections onto f and g

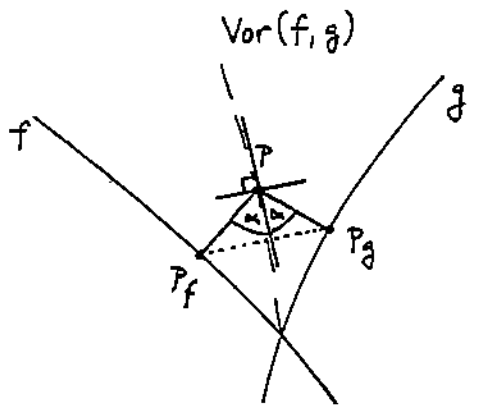

Figure 7: Tangent Plane to Voronoi Surface

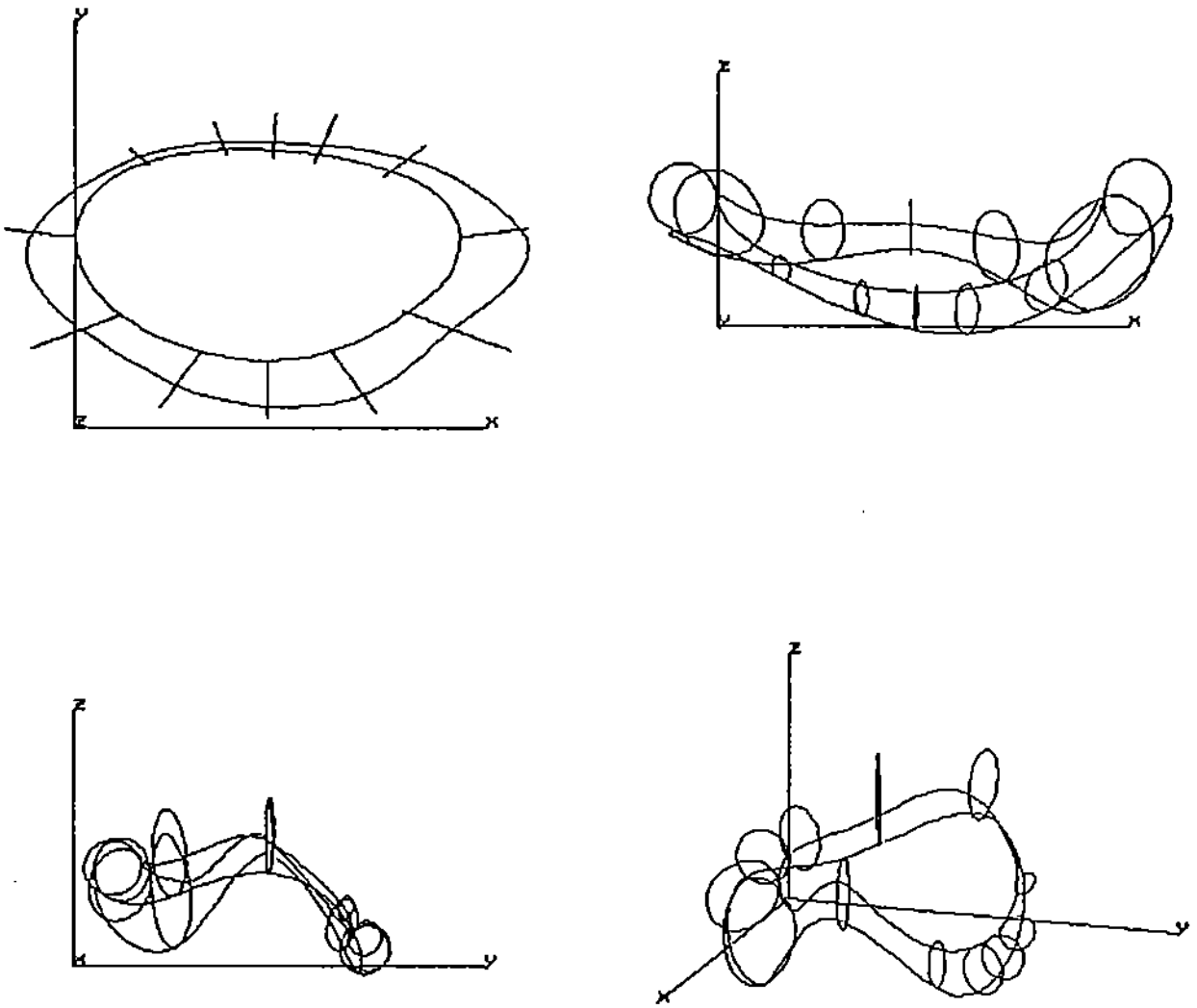

Figure 8: Sections of a Variable Radius Blend and Curves of Contact with f and g